

# Evaluation of existence region and formation time of particle accumulation structure (PAS) in half-zone liquid bridge

M. Gotoda<sup>1</sup>, T. Sano<sup>1</sup>, T. Kaneko<sup>2,3</sup>, and I. Ueno<sup>2,3</sup>

<sup>1</sup> Div. Mechanical Engineering, Graduate School of Fac. Science & Technology, Tokyo Univ. Science, 2641 Yamazaki, Noda, Chiba 278-8510, Japan

<sup>2</sup> Dept. Mechanical Engineering, Fac. Science & Technology, Tokyo Univ. Science, 2641 Yamazaki, Noda, Chiba 278-8510, Japan

<sup>3</sup> Research Institute for Science & Technology, Tokyo Univ. Science, 2641 Yamazaki, Noda, Chiba 278-8510, Japan

Received 31 July 2014 / Received in final form 16 February 2015  
Published online 8 April 2015

**Abstract.** We focused on the particle accumulation structure (PAS) produced by the thermocapillary effect in a half-zone liquid bridge. Although models of the formation of the PAS have been previously proposed, they have not been experimentally verified. An assessment of the region in which the PAS exists is very subjective and often dependent on the observer, and this has necessitated the development of an objective and quantitative evaluation method. We therefore conducted a series of experiments to verify the physical model of the particle path lines in a rotating frame of reference using the fundamental frequency of the hydrothermal wave. We evaluated the intensity of the particle accumulation based on a modification of the “accumulation measure” proposed by Kuhlmann and Muldoon (Phys. Rev. E, 2012) to objectively and quantitatively determine the existence region of the SL-1 PAS. The results of the quantitative experiment revealed that the best aspect ratio (ratio of the height to radius) of the liquid bridge for the SL-1 PAS was about 0.64, and that the PAS formation time was nearly the same as the thermal diffusion time under the considered conditions (184 words, within 200 words).

## 1 Introduction

A half-zone (HZ) liquid bridge is a geometry employed as a target for fundamental investigations on thermocapillary-driven flows. The liquid is sustained between cylindrical coaxial rods by the surface tension of the fluid to form a “bridge” between the end walls of the rods. If the liquid bridge is exposed to a temperature difference between the rods, a non-uniform distribution of the surface tension would be produced on the free surface, provided that the fluid has non-zero temperature dependency on the surface tension. This results in convective flow inside the liquid bridge. If one rod is heated and maintain at  $T_H$ , and the other at  $T_C$ , the intensity

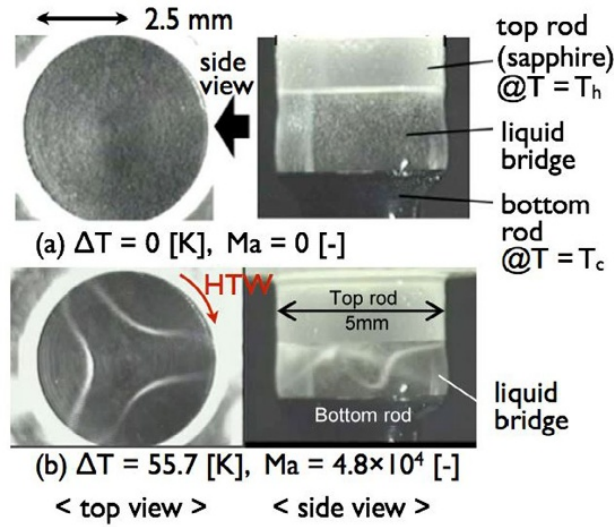


**Fig. 1.** Typical examples of the flow fields emerged in the half-zone liquid bridge observed from above and side in the cases of (a) the temperature difference  $\Delta T = 0$  [K] and corresponding  $Ma = 0$  [-] and (b)  $\Delta T = 55.7$  and  $Ma = 4.8 \times 10^4$ . In the case of (b), the PAS of the azimuthal mode number  $m = 3$  (the rotating direction of the PAS is right) is realized. The radius  $R$ , the height  $H$  and the aspect ratio  $\Gamma = H/R$  of the liquid bridge are 2.5 mm, 1.6 mm, and 0.64, respectively.

of the thermocapillary-driven flow can be described by the Marangoni number  $Ma$  as follows:

$$Ma = \frac{|\sigma_T| \Delta T \cdot H}{\rho \nu \kappa},$$

where  $\Delta T = T_H - T_C$  is the temperature difference between the two rods;  $H$  is the height of the liquid bridge (or the distance between the end walls of the rods);  $\sigma_T$  is the temperature coefficient of the surface tension  $\sigma$  of the test fluid ( $\sigma_T = \partial\sigma/\partial T$ ); and  $\rho$ ,  $\nu$ , and  $\kappa$  are the density, kinematic viscosity, and thermal diffusivity of the test fluid, respectively. The Marangoni number is a product of the thermocapillary Reynolds number  $Re$  and the Prandtl number  $Pr = \nu/\kappa$ . The shape of the liquid bridge is generally described by two parameters, namely, the aspect ratio  $\Gamma = H/R$ , where  $R$  is the radius of the rods; and the volume ratio  $V/V_0$ , where  $V$  is the volume of the liquid bridge itself, and  $V_0$  is the volume of the cylindrical space between the rods, which is given by  $\pi R^2 H$ .

The thermocapillary effect drives the fluid over the free surface from the hot-end wall to the cold-end one in a half-zone liquid bridge, and the fluid returns in the central region of the bridge toward the hot-end wall. Such a convective fluid is the basic flow pattern in the half-zone liquid bridge [1] as illustrated in Fig. 1. Especially, the convective flow inside the liquid bridge of a fluid with a moderate or large  $Pr$  exhibits transition between a two-dimensional “steady” flow shown in Fig. 1a and a three-dimensional “oscillatory” flows if the temperature difference or the Marangoni number exceeds a certain threshold [2]. The threshold of the temperature difference is referred to as the critical temperature difference  $\Delta T_c$ , whereas that of the Marangoni number is referred to as the critical Marangoni number  $Ma_c$ . This transition of the flow state is governed by the hydrothermal instability predicted by Smith & Davis [3]. There are two possible types of flow patterns near the threshold in the oscillatory state, namely, standing-wave and travelling-wave flows (Fig. 1b).

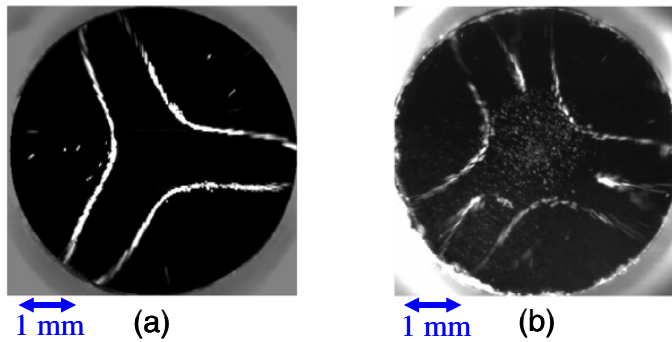


Fig. 2. Particle accumulation structure: (a) SL-1 PAS, (b) SL-2 PAS.

Schwabe et al. [4] determined the unique behaviours of particles suspended in the liquid bridge in travelling-wave-type oscillation (Fig. 1b). They observed that the particles gathered along a closed path and their solid-like structure seemed to rotate at a constant angular frequency. This behaviour of the particles is referred to as “particle accumulation structure” (PAS). The PAS was observed in the second regime of the travelling-wave flow [5,6], and was successfully reproduced by Tanaka et al. [6] in a liquid bridge with two major types of structures, namely, SL-1 PAS and SL-2 PAS, shown in Figs. 2a and b, respectively.

The mechanism of the PAS formation has been proposed by different groups. Pushkin et al. [7] proposed an inertia-dominant model based on phase locking between the flow field and the particle motions. Seki et al. [8] and Hofmann & Kuhlmann [9] proposed a model dominated by the interaction between the particles and the free surface. Although the mechanism has been discussed for a decade, a definite conclusion supported by experimental investigations is yet to be drawn.

Based on present knowledge obtained by experimental investigation, structures of the PASs [6,10] were reconstructed. Their existence regions were evaluated as a function of  $Ma$  and  $\Gamma$  [6], and the formation time of the SL-1 PAS was evaluated as a function of the particle size [1]. One of the greatest difficulties regarding the subject is the quantitative evaluation of the development of the PAS. In previous studies [1,6], the status of the PAS formation was evaluated in a subjective manner based on experience. It is thus important to develop a quantitative and objective indicator of the status of PAS formation. Recently, Kuhlmann & Muldoon [11] proposed the “accumulation measure”  $K(t)$ , which is an indication of the deviation of the particle distribution from the average in the target system. In the present study, we experimentally evaluated the occurrence condition and formation time of PAS using a modified  $K(t)$ .

## 2 Experiment

A cross-sectional view of the experimental apparatus is shown in Fig. 3. The upper rod was made from sapphire, which enabled observation of the flow field in the liquid bridge. The lower rod was made from aluminium and its edge was sharpened by machining to prevent leakage of the fluid. It was also aluminized to prevent light reflection. The liquid bridge was formed between the sustaining coaxial rods. In the present study, we employed the geometry in which the upper rod is heated and the bottom cooled after Schwabe et al. [1]; it was also convinced by ourselves that the PAS is more easily realized in the liquid bridge under this configuration. The lower-rod temperature was fixed at 20°C and the upper-rod temperature was varied to change the

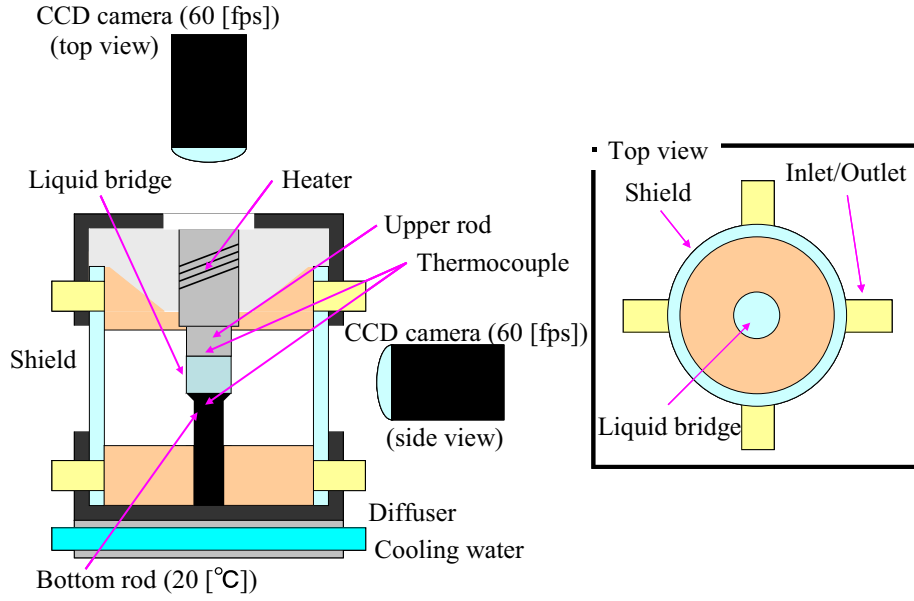


**Fig. 3.** Cross-sectional and top views of experimental apparatus.

temperature difference between the sustaining rods. The behaviour of the particles was recorded from the top and the side by two CCD cameras. An ambient gas region was formed inside the external coaxial shield surrounding the liquid bridge, and there was a null ambient forced gas flow (that is,  $Re_{amb} = 0$ ).

The test fluid used for the liquid bridge was silicone oil, which has a kinetic viscosity of 2 cSt and Prandtl number of 28.1 at room temperature. Gold-coated acrylic particles of diameter 15 microns were put inside the liquid bridge to facilitate visualization of the convection in the liquid bridge. This kind of particle was examined for more than a year to diverse in the fluid without any segregation, and was employed in the on-orbit experiments of the thermocapillary-driven flow known as “Marangoni Experiment in Space (MEIS)” in the Japan Experiment Module “Kibo” aboard the International Space Station. The particle is a well-shaped sphere so that one can avoid the effect of the shape of the particles to trace the flow field. The density ratio  $\rho_p/\rho_f$  was 2.0 and the Stokes number  $St(= 2\rho_p R_p^2/9\rho_f H^2)$  [9] was in the range of  $8.6 \times 10^{-6}$  to  $12.8 \times 10^{-6}$ . The radius  $R$  of the liquid bridge was fixed at 2.5 mm and the height  $H$  was varied to change the aspect ratio  $\Gamma = H/R$  of the liquid bridge. The volume ratio of the liquid bridge,  $V/V_0$ , was maintained constant at 1.0. The experiment was repeated for four different aspect ratios  $\Gamma$  of 0.56, 0.60, 0.64, and 0.68, and Marangoni numbers ranging between  $2.5 \times 10^4$  and  $4.5 \times 10^4$ .

An external shield [12] with an inner diameter of 25 mm ( $= 5R$ ) was fabricated and used to define the thermal boundary. The shield was set coaxially with the sustaining rods around the liquid bridge. The corresponding gap between the surface of the liquid bridge and the inner surface of the external shield was 10 mm ( $= 2R$ ). We evaluated the region in which the PAS existed and the formation time based on the “accumulation measure” proposed by Kuhlmann and Muldoon [11], given by

$$K(t) = \frac{1}{2(N_p - \bar{N})} \sum_{i=1}^{N_{cells}} |N_i(t) - \bar{N}|.$$

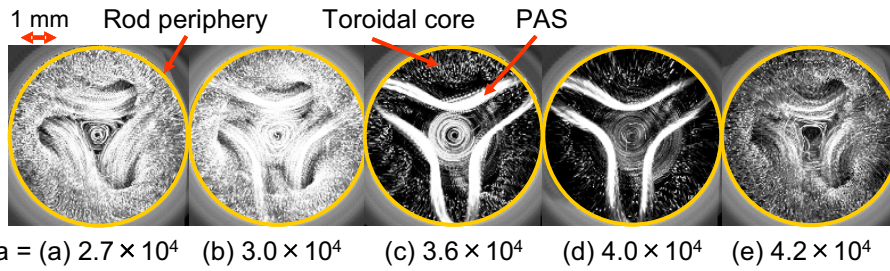


**Fig. 4.** Typical flow patterns observed from the top. The external shield diameter and aspect ratio were 25 mm and 0.64, respectively. Each image was obtained by 1 s accumulation in the rotating frame of reference using the fundamental frequency of the hydrothermal wave.

It is difficult to determine the number of particles, so we modified the equation for our experiment.  $N_p$  is the number of particle pixels (the white part),  $\bar{N}$  is the average number of particle pixels in each cell,  $N_i(t)$  is the number of particle pixels in the  $i$ -th cell at time  $t$ , and  $N_{cells}$  is the total number of cells. Kuhlmann and Muldoon [11] radially divided the liquid bridge into three-dimensional cells of equal volume. We, however, divided the image as observed from the top into equal two-dimensional rectangular cells and evaluated the  $K(t)$  value.

Firstly, we determined the number of particle pixels  $N_p$  from the luminance, and calculated the average number of particle pixels  $\bar{N}$  per cell. Secondly, we determined the number of particle pixels  $N_i(t)$  and summed the absolute value of  $N_i(t) - \bar{N}$  for each cell. We confirmed that when the particles are dispersed,  $K(t)$  would be close to 0, and when the particles are concentrated in a single cell,  $K(t)$  would be close to 1. The adopted experimental method is basically the same as that of Schwabe et al. [1], and the homogenous dispersal of the particle was realised by stirring the liquid bridge with a thin wire after full development of the flow field at a certain temperature difference. We defined time zero as when the wire was removed from the liquid bridge and evaluated  $K(t)$  for each time step.

### 3 Results and discussion

PAS occurs when there is a large temperature difference across a liquid bridge. Special attention was given to SL-1 PAS in our experiment.

Figure 4 shows the top views of the particle path lines over 1 s in the rotating frame of reference using the fundamental frequency of the hydrothermal wave for each Marangoni number and  $\Gamma = 0.64$ . Each image was obtained by accumulating the pictures recorded for 2 min after stirring the liquid bridge. Clearly observable from the images are the triangular particle depletion zone at  $\text{Ma} = 2.7 \times 10^4$ , the appearance of SL-1 PAS, and the “toroidal core” at  $\text{Ma} = 3.6 \times 10^4$ . We also confirmed the vanishing of SL-1 PAS at  $\text{Ma} = 4.2 \times 10^4$ , and the flow field at  $\text{Ma} = 4.2 \times 10^4$  was similar to that at  $\text{Ma} = 2.7 \times 10^4$ . Hence, we were able to reproduce the results of the model of Kuhlmann et al. [13] by our experimental approach. We detected the PAS in these images; however, to quantitatively determine the region in which the PAS existed, we evaluated the intensity of the particle accumulation using the “accumulation measure” proposed by Kuhlmann & Muldoon [11].

Figure 5 shows  $K(t)$  as a function of the non-dimensional time for  $\text{Ma} = 2.7 \times 10^4$ ,  $3.6 \times 10^4$ , and  $4.2 \times 10^4$ , under  $\Gamma = 0.64$ . The non-dimensional time  $t^*$  is defined by dividing the real time  $t$  by the thermal diffusion time  $\tau (= H^2/\kappa)$ . When the PAS appeared at  $\text{Ma} = 3.6 \times 10^4$ ,  $K(t)$  increased rapidly shortly after stirring the liquid

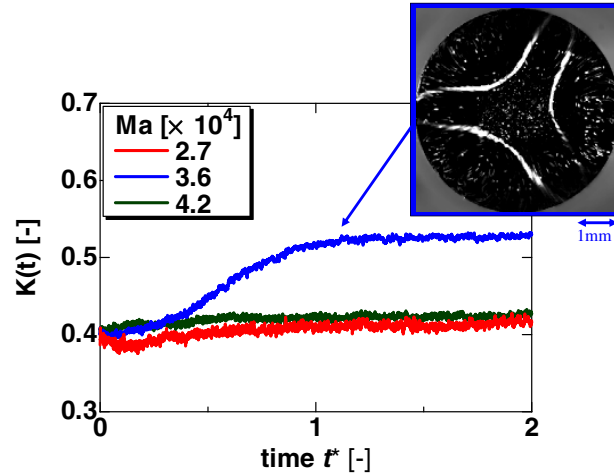


**Fig. 5.**  $K(t)$  as a function of the non-dimensional time for  $Ma = 2.7 \times 10^4$ ,  $3.6 \times 10^4$ , and  $4.2 \times 10^4$ , and  $\Gamma = 0.64$ .

bridge, and finally converged to a constant value. When the PAS did not appear, there was no significant increase in  $K(t)$  after stirring. We denote the convergence value for each Marangoni number by  $K_c$ . We also define the formation time when  $K(t)$  becomes constant.

Figure 6 shows the graph of  $Ma$  versus  $K_c$  for aspect ratio  $\Gamma = 0.56, 0.60, 0.64$ , and  $0.68$ . It can be observed that, for an aspect ratio of  $0.64$ , with increasing Marangoni number  $Ma$ ,  $K_c$  increases from a constant value around  $Ma = 2.7 \times 10^4$ , attains another constant value, and then begins to decrease again around  $Ma = 4.2 \times 10^4$ . From the experimental results, we deduce that the PAS appeared at  $Ma = 2.7 \times 10^4$ , and disappeared at  $Ma = 4.2 \times 10^4$ . The tendencies were the same for aspect ratios of  $0.56$  and  $0.60$ . However, for an aspect ratio of  $0.68$ ,  $K_c$  was constant over the considered range of  $Ma$  values, and no PAS could be observed with the naked eye. Mukin and Kuhlmann [14] proposed that the PAS is formed on/along the KAM torus in the flow field in the liquid bridge; the particles in the chaotic streamlines interact with free surface to change their trajectory from the chaotic streamline to KAM torii as the regular trajectories in the bridge. And the shape of regular and the chaotic streamlines are sensitive to the liquid-bridge shape in the terms of the aspect ratio and volume ratio. We conducted a series of experiments by varying the liquid-bridge aspect ratio from  $0.56$  to  $0.68$ . It is found that the PAS is formed in the cases of  $\Gamma$  from  $0.56$  to  $0.64$ , and never formed in the cases of  $\Gamma = 0.68$ . This might be explained by considering that the closed KAM torii of the azimuthal wave number  $m = 3$  never formed under  $\Gamma = 0.68$ .

Figure 7 shows the instantaneous field of the top views of the liquid bridge at  $Ma = 2.7 \times 10^4$  for each considered value of the aspect ratio. It is very difficult to determine the differences among the images by the naked eye, but this can be clearly done using  $K_c$ , and the differences can be attributed to the size of the particle depletion zone.

Figure 8 shows the contour graph of  $K_c$ . The different colours in the graph are used to highlight the  $K_c$  values. Red indicates accumulation of particles whereas blue indicates dispersion of particles. From the graph, it can be seen that the best aspect ratio for PAS formation under the present conditions is about  $0.64$ .

Figure 9 shows the non-dimensional formation time versus the Marangoni number ( $3.0 \times 10^4$  to  $4.0 \times 10^4$ ) for PAS aspect ratio  $\Gamma = 0.56, 0.60$ , and  $0.64$ . In a previous

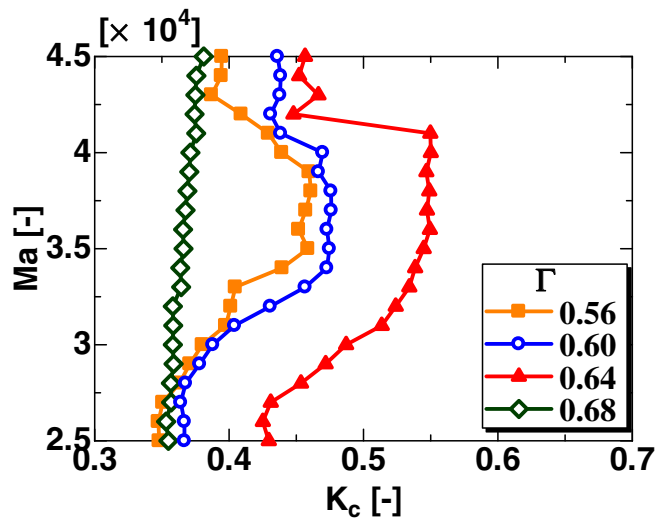


Fig. 6.  $Ma$  versus  $K_c$  for  $\Gamma = 0.56, 0.60, 0.64,$  and  $0.68$ .

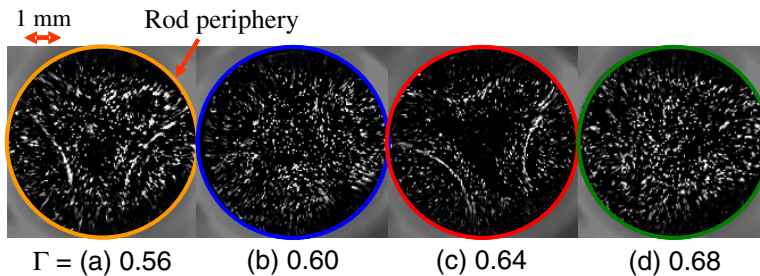


Fig. 7. Typical top views of the liquid bridge for  $Ma = 2.7 \times 10^4$  and aspect ratio  $\Gamma = 0.56, 0.60, 0.64,$  and  $0.68$ .

study [11], the formation time was non-dimensionalised by the viscous momentum diffusion time  $\tau(= H^2/\nu)$ . This was because the particles inside the liquid bridge were considered to be carried by the motion of the fluid. However, in the present study, we non-dimensionalised the formation time by the thermal diffusion time  $\tau(= H^2/\kappa)$ , and found that the formation time was nearly unity in most cases. This means that the particles inside the liquid bridge were not only carried by the motion of the fluid. Perfect de-mixing was achieved at the same time as the full development of the flow field owing to thermal diffusion. That is, it is indispensable of the fully-developed traveling-type HTW to the formation of the PAS. In the figure we also plot the formation time for the particles of smaller  $St$  in the case of  $Ma = 3.6 \times 10^4$ , and it is found that the formation time becomes moderately longer with the smaller  $St$  particles. Such tendency agrees qualitatively with Muldoon & Kuhlmann [15], although their formation time corresponds to the time of the particle behaviours starting from the fully-developed flow field in the bridge. We pay attention to the formation time and their variation due to the change of the particle density. Kuhlmann & Muldoon [11] made comparisons of the formation times of the PAS by considering the different physical models. The formation time of the PAS by considering the inertia effect only [7] becomes much longer than that by considering the particle-free surface interaction as well as the inertia effect [9]. In addition, the sensitivity of the formation time to the particle density becomes much less in the case of the

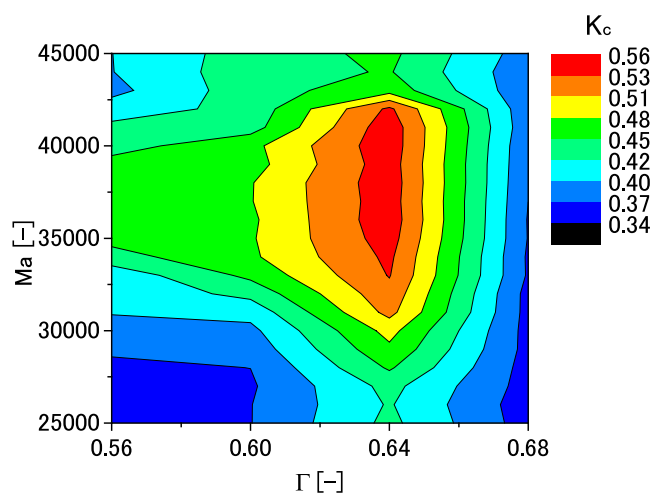


Fig. 8. Contour graph of  $K_c$ . The diameter of the external shield was 25 mm.

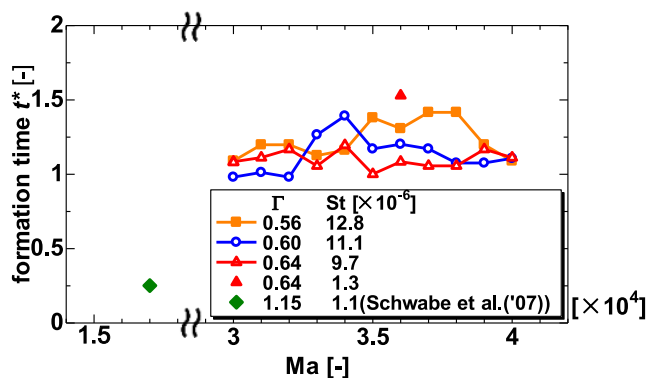


Fig. 9. Non-dimensional PAS formation time versus thermal diffusion time for aspect ratio  $\Gamma = 0.56, 0.60,$  and  $0.64$ .

model considering the both of inertia and the particle-free surface interaction. The present results indicate the similar trends in both of the formation time itself and its sensitivity to the particle density. Figure 9 also includes the result of Schwabe et al. [1], obtained under the conditions of  $\Gamma = 1.15$ ,  $\Delta T = 38.0[\text{K}]$  ( $\text{Ma} = 1.7 \times 10^4$ ),  $\text{Pr} = 8$ , and  $\text{St} = 1.1 \times 10^{-6}$ . Compared to our results, significant difference can be observed, which is because the two experiments were conducted using different Marangoni numbers, Prandtl numbers, and Stokes numbers. Further study is therefore required for a full understanding of what determines the PAS formation time.

## 4 Conclusion

We gave special attention to the region in which the PAS appeared and the formation time of SL-1 PAS. We found that we could reproduce the results of the physical model proposed by Kuhlmann et al. [13] of the particle depletion zone and “toroidal core” from our obtained images in the rotating frame of reference using the fundamental frequency of the hydrothermal wave. We could also objectively and quantitatively



determine the region in which the PAS existed using a modification of the “accumulation measure”. Furthermore, we found that the PAS formation time was nearly the same as the thermal diffusion time under the considered conditions. We compared our results with those of a previous study on the PAS formation time and observed significant difference, which could be attributed to the different experimental conditions. Hence, further study is required to verify the determined PAS formation time and the relationship between it and the thermal diffusion time.

We acknowledge support from JSPS through a Grant-in-Aid for Scientific Research (B) (project number 24360078). This work was performed in preparation for the Japanese-European Research Experiments on Marangoni Instabilities (JEREMI). The authors gratefully acknowledge the contributions of the project members through discussions.

## References

1. D. Schwabe, A.I. Mizev, M. Udayasankar, S. Tanaka, *Phys. Fluids* **19**, 072101 (2007)
2. F. Preisser, D. Schwabe, A. Scharmann, *J. Fluid Mech.* **126**, 545 (1983)
3. M.K. Smith, S.H. Davis, *J. Fluid Mech.* **132**, 119 (1983)
4. D. Schwabe, P. Hintz, S. Flank, *Microgravity Sci. Technol.* **9**, 163 (1996)
5. I. Ueno, S. Tanaka, H. Kawamura, *Phys. Fluid* **15**, 408 (2003)
6. S. Tanaka, H. Kawamura, I. Ueno, D. Schwabe, *Phys. Fluids* **18**, 067103 (2006)
7. D.O. Pushkin, D.E. Melnikov, V.M. Shevtsova, *Phys. Rev. Lett.* **106**, 234501–1 (2011)
8. T. Seki, S. Tanaka, H. Kawamura, 6th Japan/China Workshop on Microgravity Science, 41-42 (2005)
9. E. Hofmann, H.C. Kuhlmann, *Phys. Fluids* **23**, 072106 (2011)
10. Y. Niigaki, I. Ueno, *Transaction of the Japan Society for Aeronautical and Space Sciences, Aerospace Technology* **10**, Ph\_score 33-Ph\_37 (2012)
11. H.C. Kuhlmann, F.H. Muldoon, *Phys. Rev. E* **85**, 046310 (2012)
12. I. Ueno, A. Kawazoe, H. Enomoto, *Fluid Dyn. Mater. Process.* **6** (2010)
13. H.C. Kuhlmann, R.V. Mukin, T. Sano, I. Ueno, *Fluid Dyn. Res.*, 041421 (2014)
14. R.V. Mukin, H.C. Kuhlmann, *Phys. Rev. E* **88**, 053016-1–053016-20 (2013)
15. F.H. Muldoon, H.C. Kuhlmann, *Physica D* **253**, 40 (2013)